Aceh Int. J. Sci. Technol., 9(3) 197-206
December 2020
doi: 10.13170/18256

Aceh International Journal of Science and Technology
ISSN: p-2088-9860; e-2503-2398
Journal homepage: http://jurnal.unsyiah.ac.id/aijst

Adsorption of Cd(II) Ions From Aqueous Solution By A Low-Cost Biosorbent Prepared From Ipomea Pes-Caprae Stem

Thaharah Ramadhani[1], Faisal Abdullah[1], Indra Indra[1], Abrar Muslim[2*], Suhendrayatna Suhendrayatna[2], Hesti Meilina[2], Saiful Saiful[3]

[1]Integrated Coastal Resource Management Magister Study Program, Postgraduate Program, Universitas Syiah Kuala, Indonesia
[2]Department of Chemical Engineering, Faculty of Engineering, Universitas Syiah Kuala, Indonesia
[3]Department of Chemistry, Faculty of Mathematics and Science, Universitas Syiah Kuala, Indonesia
*Corresponding author email: abrar.muslim@che.unsyiah.ac.id

Received : October 8, 2020
Accepted : November 1, 2020
Online : December 30, 2020

Abstract – The use of a low-cost biosorbent prepared from Ipomoea pes-caprae stem for the adsorption of Cd(II) ions from aqueous solution at different contact times, biosorbent sizes, pH values, and initial Cd(II) ions concentration solution was investigated. The biosorbent was analyzed using Fourier-transform infrared spectroscopy (FT-IR) to find important IR-active functional groups. A scanning electron microscope (SEM) was used to examine the biosorbent morphology. The experimental results showed the highest Cd(II) ions adsorption was 29.513 mg/g under an optimal condition as initial Cd(II) ions concentration of 662.77 mg/L, 1 g dose, 80-min contact time, pH 5, 75 rpm of stirring speed, 1 atm, and 30 ^{o}C. Based on the optimal condition, Cd(II) ions' adsorption kinetics obeys the linearized pseudo-second-order kinetics (R^2 = 0.996), and the adsorption capacity and rate attained was 44.444 mg/g and 0.097 g/mg. Min, respectively. Besides, the adsorption isotherms were very well fitted by the linearized Langmuir isotherm model, and the monolayer adsorption capacity and pore volume determined was 30.121 mg/g and 0.129 L/mg, respectively. These results indicated the chemisorption nature.

Keywords: Ipomea pes-caprae, biosorbent, adsorption, kinetic, isotherm.

Introduction

The coastal area might be influenced by human activities, including marine transportation, offshore oil production, urban, agricultural, and industrial processes. Pollutants such as heavy metals in the water will be harmful to the organism's life, which indirectly impacts human health. One type of heavy metal that is in the waters and is toxic is the metal Cadmium. In coastal areas, Cadmium metal pollution mostly originates from landfill and rainwater flow of by-product of mining, casting zinc, copper, or tin, which is widely used in various industries, especially in electrode plates, painting, alloys (alloys), pigments, stabilizers in battery and plastic factories (Rao *et al.*, 2010). Sea transportation activities, including ship repair activities, also contributed to Cd(II) ions pollution of the coastal area (Dominggus, 2011). Cadmium toxicity can affect the human body, such as vesicular trafficking, cytoskeleton, and cell wall reconstruction (Wan and Zhang, 2012).

Many methods can be applied to reduce the concentration of heavy metals in wastewater, such as mechanical filtration, oxidation-reduction of chemical deposition, ion exchange, and adsorption. Among others, adsorption is a promising method because the process is more effective, efficient, and cheaper (Dimple, 2014). Low-cost bio sorbents had been proposed for Cd(II) ions adsorption, which were prepared from sawdust and rice husk (Nahar *et al.*, 2018), corn cob (Mahmood-ul-Hassan *et al.*, 2015), olive oil by-products (Anastopoulos *et al.*, 2015), livestock waste (Zhang *et al.*, 2017) and by-products and waste from the forest (Cutillas-Barreiro *et al.*, 2016).

Ipomoea pes-caprae, which is waste from the coastal forest, was used in bioaccumulation of Pb, Zn, As, Se, Cr, and Ni, wherein the metal ions were expected to be bounded with its chemical compounds (Kozak *et al.*, 2015). The Ipomoea leaves and stem might be a promising biosorbent because several species of Ipomoea, including Ipomoea pes-caprae, have functional groups of hydroxyl (O-H) such glycolipids (Hernandez-Carlos *et al.*, 1999), glycosides (Pareda-Mirinda *et al.*, 2005, Rosas-Ramírez and Pereda-Miranda, 2013), sterols and ester (C=O) such as isochlorogenic acids (Teramachi *et al.*, 2005, Batiga *et al.*, 2019). Therefore, it is necessary to utilize it as a biosorbent since it has some functional groups to be active sites for Cd(II) ions adsorption.

The purpose of this study was to utilize biosorbent from Ipomea pes-caprae stem (BIPS) for the adsorption of Cd(II) ions in an Aqueous Solution. The functional groups and physical morphology of the BIPS were investigated using FTIR and SEM analyses. The effect of independent variables, i.e., contact time, the BIPS size, pH, and initial aqueous Cd(II) ions concentration on the BIPS adsorption capacity were investigated, and the adsorption kinetics and adsorption isotherms were obtained.

Materials and Methods

Material

The Coastal Plant Ipomea Pes-Caprae Stems, which were taken from Peukan Bada area of Aceh Besar District, was used as raw material to utilize the biosorbent. Ipomea Pes-Caprae stems were sliced small, then washed thoroughly using tap water, dried in the oven at a temperature of 150 ˚C for 8 hours until the sliced stems weigh being constant. The dried material was then crushed to powder. Biosorbent of Ipomea Pes-Caprae Stems (BIPS) was then divided into 4 (four) sizes, namely: BIPS-A < 230 mesh, 230 < BIPS-B < 120 mesh, 120 < BIPS-C < 60 mesh, and BIPS-D > 60 mesh. Fourier transform infrared spectroscopy (FTIR, Shimadzu Type FTIR-8400, Japan) was used to identify the functional groups of the BIPS. Scanning Electron Microscopy (SEM) (Hitachi Type TM-3000, 500VA, 1 phase 50/60Hz, Japan) was used to investigate the physical morphology of the BIPS.

$Cd(NO_3)_2.4H_2O$ (Sigma-Aldrich, 99%) and aquadest (distilled water) were used to prepare the Cd(II) ions aqueous solution. 1 (one) L of a stock Cd(II) ions aqueous solution was made with a concentration of 1000 mg/L. It was diluted according to predetermined Cd(II) ions concentration in the range of 5-650 mg/L which was in the range of 5-1000 mg/L (Kurniawan et. al. 2006), but the real concentration obtained was to be 662.77; 255.34; 110.13; 51.26; 23.4 and 4.99 mg/L based on Atomic Absorption Spectroscopy (AAS) analysis.

Adsorption Experimental Method

A preliminary adsorption experiment in batch mode was conducted to obtain equilibrium time (Muslim *et al.*, 2015). The BIPS-A was used because it was smallest size and expected to have higher adsorption capacity. The BIPS-A and Cd(II) ions adsorption system consisted of 1 g of BIPS-A, 100 mL of Cd(II) ions solution at 662.77 mg/L. It was stirred at 75 rpm, 1 atm and 30 ˚C. The solution samples of 2-mL were taken at the contact time of 0, 20, 40, 60, 80 min using variable volume pipettes. Based on the procedure in the previous study (Muslim, 2017), the samples were diluted with 10 mL of distilled water and shacked in 15-mL vial. The filtrate was then separated by filtering using syringe filter, and then analyzed using the AAS.

Based on the preliminary adsorption experiment whereas equilibrium time was obtained, the effect of independent variables were investigated. The experimental procedure of the design variable in the previous study was taken into account (Muslim *et al.*, 2017a). The range of independent variables was 0–80 min of contact time, biosorbent with various sizes, 4.99–662.77mg/L of initial aqueous Cd(II) ions concentration, pH 3–5 with a dose of 1 g at 1 atm and 30 ˚C. The Cd(II) aqueous solution pH was adjusted by dropping NaOH and HCl aqueous solution with the concentration at the range of 0.01-0.5 M prepared from the stock solutions (99% pure from Aldrich); the solution pH was measured using Cobra3 Chem-Unit (PHYWE type 12153.00, Western Germany). Adsorption capacity over contact time was obtained using Equation (1):

$$q_t = \frac{(C_0 - C_n)V_S}{m_{AC}} \tag{1}$$

where C_0 and C_n (mg/L) are the aqueous Cd(II) ions concentration at the time of 0 and t (min), respectively; q_t is the adsorption capacity the time of t; V_S (L) is as the solution volume (L); and m_{AC} (g) is the biosorbent mass.

Results

Functional groups of biosorbent

Figure 1 shows the transmission spectrum of the biosorbent. The strong band at 3530–3725 cm -1 of wavenumber with the peak at 3631.96 cm -1 with the transmittance of 95.3% is associated to the O-H stretch of hydroxyl group such as phenol compound, alcohol monomer and hydrogen (Lee *et al.*, 2015). A band at 3780–3015 cm -1, which has two peaks at 2920.23 and 2862.72 cm -1, is assigned to the C–H stretch of alkenes (Chakravarty *et al.*, 2010), and the transmittance was 86.72% and 87.14%, respectively. A sharp band at 1730–1735 cm -1 with a peak at 1734.01 cm -1 is assigned to the C=O stretch of carbonyls. There is the N–O asymmetric stretching of nitro compounds at 1472–1557 cm -1 with two peaks at 1425.40 and 1510.29 cm -1 . The last one is a wide band of C–N stretch at 902–1200 cm -1 is associated with aliphatic amines with two peaks at 1012.83 and 1031.92 cm -1 (Chakravarty *et al.*, 2010, Muslim *et al.*, 2017a).

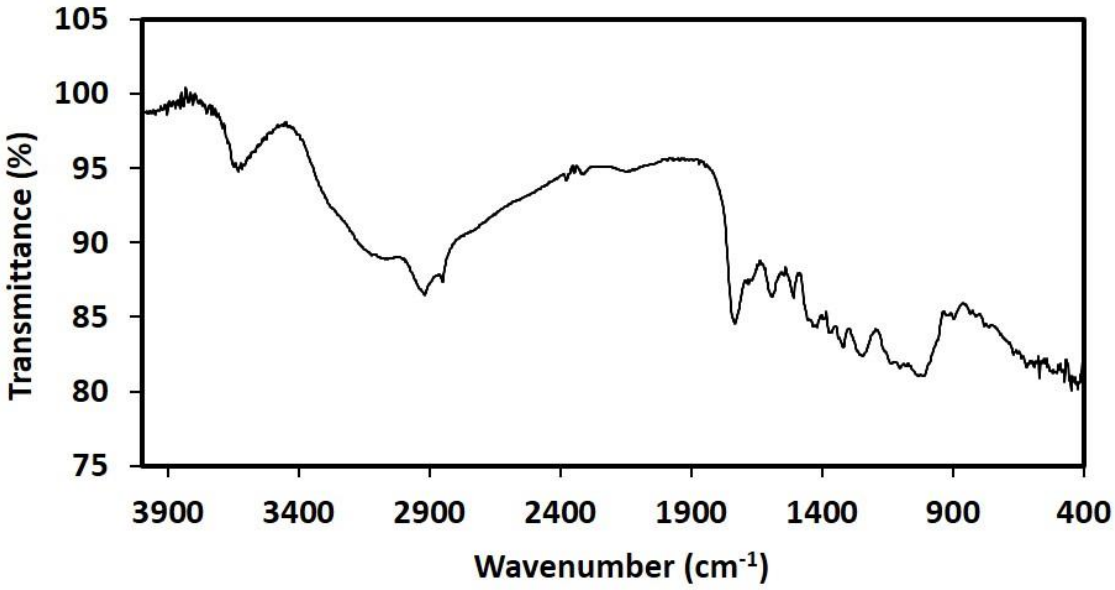

Figure 1. The FTIR spectra of the BIPS-A

Surface morphology of biosorbent

Physical morphology of the BIPS-A and BIPS-C by the SEM analysis are shown in Figures 2(a) and 2(b), respectively. As can be seen in Figures 2(a) and 2(b), the pores on the biosorbent are uneven and irregular. However, there are some differences between the two biosorbent due to the different size of both the BIPS-A and BIPS-C. The BIPS-A has more opened and bigger pores, and there are more pores on the BIPS-A compared to the BIPS-C.

Effect of contact time

The effect of contact time on the Cd(II) ions adsorption capacity of the biosorbent is shown in Figure 3(a). The experiments were conducted under a condition as 1 g of biosorbent , 662.77mg/L of initial aqueous Cd(II) ions concentration, pH 5, 1 atm and 30 ^{o}C. The adsorption capacity for the BIPS-A was 24.179, 23.591, 29.632 and 29.513 mg/g at 20, 40, 60 and 80 min, respectively. Meanwhile, it was 16.472, 22.198, 21.827 and 23.003 mg/g for the BIPS-B, and it was 2.409, 7.064, 19.482, and 19.202 mg/g for the BIPS-C, respectively. It increased sharply in the first 20 min of contact time for the BIPS-A and BIP-B, and it increased gradually to reach an equilibrium time of 80 min. However, adsorption capacity for the BIPS-C increased gradually in the beginning 40 min of contact time, and it inclined considerably until reaching the equilibrium time of 80 min.

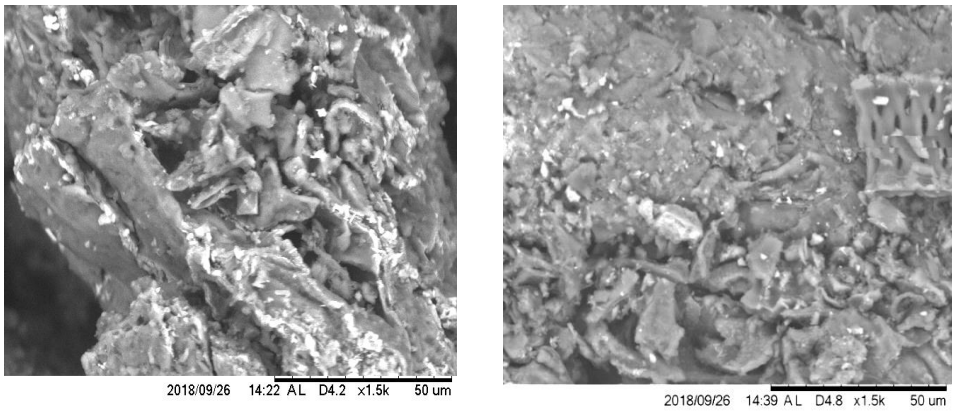

(a) (b)

Figure 2. The SEM micrographs of (a) the BIPS-A and (b) the BIPS-C at 1500x magnification

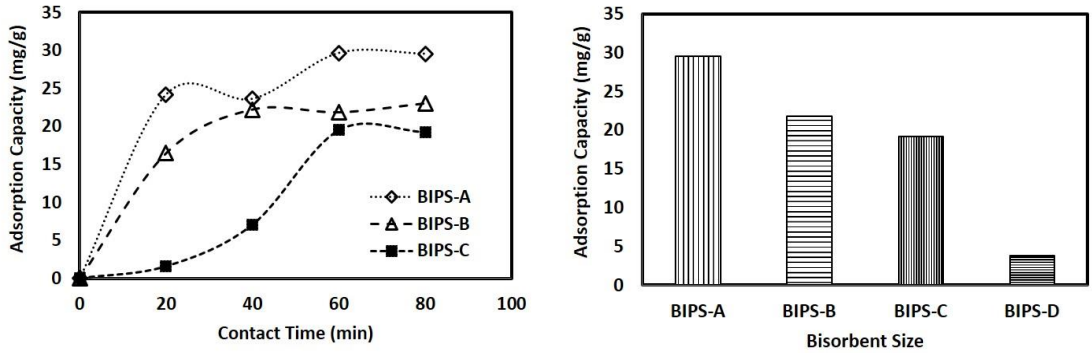

(a) (b)

Figure 3. Effect of (a) contact time and (b) biosorbent size on adsorption capacity

Effect of biosorbent size

Figure 3(b) illustrates biosorbent BIPS-A, BIPS-B, BIPS-C, and BIPS-D presenting the size of less than 230 mesh (0.063 mm), in range of 230-120 mesh, in range of 120-60 mesh and more than 60 mesh, respectively with the set dependent variables (1 g of dose, 662.77mg/L of initial aqueous Cd(II) ions concentration, pH 5, 1 atm and 30 °C). As viewed in Figure 3(b), the adsorption capacity inclined significantly from 3.795 to 29.513 mg/g by reducing the biosorbent size from D size to C size. It increased continuously to be 21.827 and 29.513 mg/g for size B and A, respectively.

Effect of pH

Figure 4(a) shows a linear increase of adsorption capacity in the pH range of 3-5 with a maximum Cd(II) ions being adsorbed by the BIPS-A at pH of 5 with the set dependent variables (1 g of BIPS-A, 662.77mg/L of initial aqueous Cd(II) ions concentration, 1 atm, and 30 °C). The adsorption capacity was 26.349, 28.379, and 29.513 mg/g at pH of 3, 4, and 5, respectively.

Effect of initial Cd(II) ions concentration

Figure 4(b) demonstrations the adsorption capacity of BIPS-A over initial Cd(II) concentration in the range of 4.99-662.77 mg/L with the set dependent variables (1 g of BIPS-A, 662.77mg/L of initial aqueous Cd(II) ions concentration, pH 5, 1 atm and 30 °C). It increased gradually from 0.498 to 2.339, 4.9650, and 9.893 mg/g at 4.99 to 23.41, 51.26, and 110.13, respectively. When initial Cd(II) ions concentration was changed to 255.34, it increased a bit sharp to 23.014 mg/g, and it was back to increase gradually to 29.513 mg/g at 662.77 mg/L.

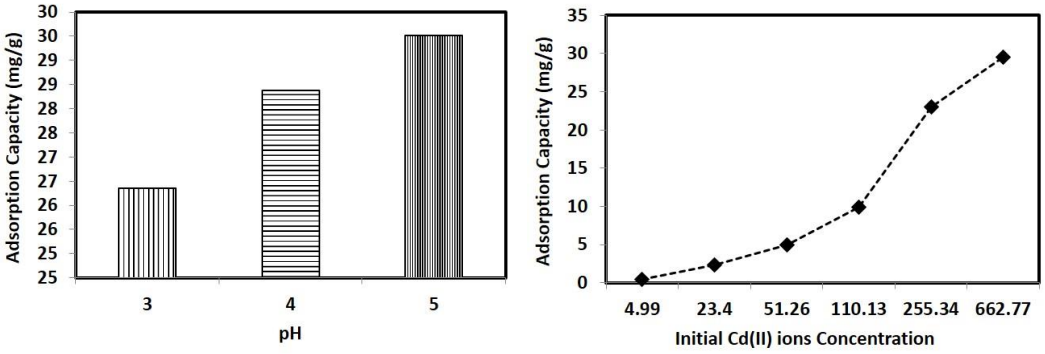

(a) (b)

Figure 4. Adsorption capacity over (a) pH and (b) initial Cd(II) ions concentration.

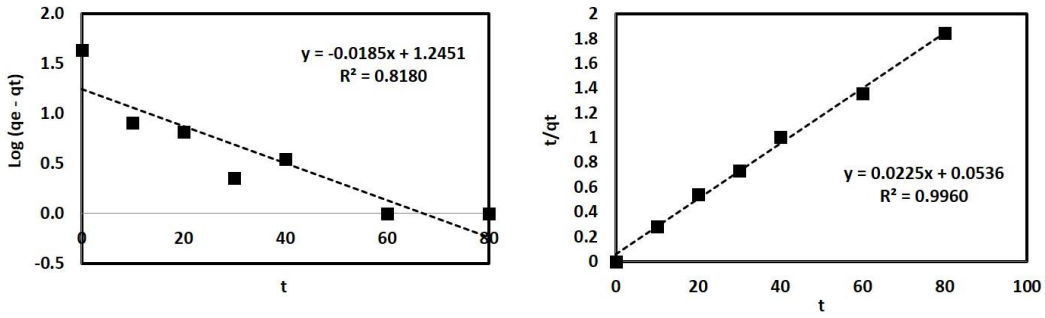

(a) (b)

Figure 5. Plots of linearized (a) Lagergren model and (b) Ho model for adsorption kinetic

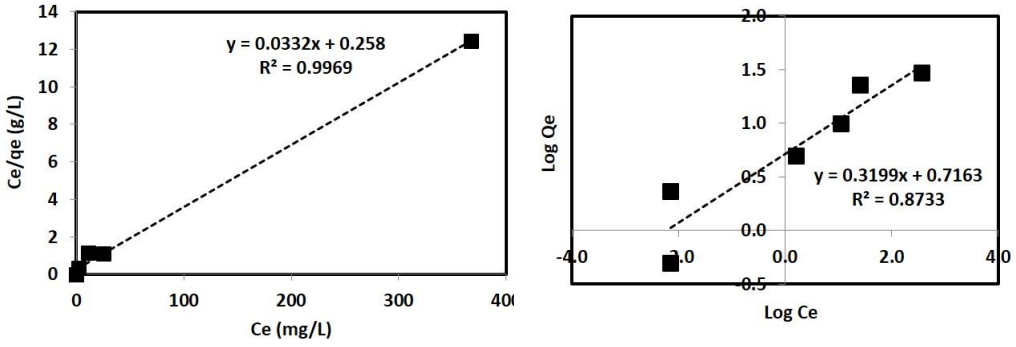

(a) (b)

Figure 6. Plots of linearized (a) Langmuir model and (b) Freundlich model for adsorption isotherm

Adsorption kinetic and isotherm

The linearized form of Lagergren and Ho models (Lagergren, 1989, Ho *et al.*, 1996) for adsorption kinetic presenting the pseudo first-order (PFO) and pseudo second-order (PSO) kinetic, respectively, were used to obtain the kinetic adsorption parameters, which can be expressed as Equations (2) and (3), respectively:

$$\log(q_e - q_t) = \log q_e - \left(\frac{k_L t}{2.303}\right) \quad (2)$$

$$\frac{t}{q_t} = \frac{1}{k_H q_e^{\,2}} + \frac{t}{q_e} \quad (3)$$

where q_t and q_e (mg/g) are adsorption capacity at time of t (min) and equilibrium time, respectively; and k_L (/min) and k_H (g/mg.min) are the PFO and PSO kinetic rate constants, respectively. All the adsorption kinetic values were determined using the slope and intercept of Figures 5(a) and 5(b) (Muslim *et al*., 2017b).

To determine the adsorption isotherm parameters, linearized form of Langmuir and Freundlich models (Langmuir, 1918, Freundlich, 1906) were taken into account to obtain the adsorption kinetic parameters, which are Equations (4) and (5), respectively:

$$\frac{C_e}{q_e} = \frac{1}{q_m K_L} + \frac{1}{q_m} C_e \tag{4}$$

$$\log q_e = \frac{1}{n} \log C_e + \log K_F \tag{5}$$

where q_m (mg/g) is Langmuir monolayer adsorption capacity; K_L (L/mg) and K_F (mg/g) denotes as Langmuir constant of pore volume and Freundlich constant of adsorption capacity, respectively; and 1/n denotes the adsorption intensity. All the adsorption kinetic values were determined using the slope and intercept of Figures 6(a) and 5(b).

Discussions

Functional groups of biosorbent

The BIPS-A transmission spectrum only was analyzed by the FT-IR because this biosorbent showed the highest adsorption capacity compared to other biosorbents, which will be highlighted in further results. As highlighted in the FT-IR result, the biosorbent had some active functional groups, such as hydroxyl group (O-H), glycolipids, and glycosides (Hernandez-Carlos *et al*., 1999, Pareda-Mirinda *et al*., 2005, Rosas-Ramírez and Pereda-Miranda, 2013). The biosorbent had also carbonyls (C=O), which would be isochlorogenic acids (Teramachi *et al*., 2005, Batiga *et al*., 2019). These functional groups together with the other ones such as alkenes (C–H), nitro compounds (N–O) and amines (C–N) on the surface of biosorbent, should play an important role in the adsorption of Cd(II) ions onto the biosorbent.

Surface morphology of biosorbent

A comparison to the surface morphology BIPS-A, which had the highest adsorption capacity, has one of biosorbents only, the BIPS-C, to be discussed. As highlighted in the results, the BIPS-A has more opened and larger pores, and there are more pores on the BIPS-A compared to the BIPS-C. This result was reasonable because crushing the biosorbent of BIPS-C to smaller size might break the BIPS-C surface including the pores, and it might close the pores. This reason is because of collision, friction, impingement and shear, resulting not only particle size reduction but also the porosity breakdown (Zorica *et al*., 2019) and broken edger of pores becoming closed pores (Lee *et al*., 2019).

Effect of contact time

As viewed in Figure 3(a), the first 20-min contact time for the BIPS-A and BIP-B should be the initial stage of Cd(II) ions adsorption onto the biosorbent. The initial stage of adsorption is generally controlled by the diffusion of adsorbate in the aqueous phase to the solid phase on the biosorbent. The same interpretation was also reported for adsorption of Cu(II) ions onto biosorbent prepared from Thevetia peruviana leaf powder (Medhi *et al*., 2020). Therefore, the adsorption capacity of BIPS-A and BIP-B increased sharply for the first 20min contact time. However, it was different for the BIPS-C because the biosorbent had less porosity, as highlighted in the FTIR results, leading to less diffusion of adsorbate in the aqueous phase to the solid phase.

The biosorbent adsorption capacity increased slowly after 20-min contact time because of slow intraparticle diffusion between Cd(II) ions and the biosorbent. Cd(II) ions adsorption should be driven by the intraparticle interactions, such as Van der Waals interaction, electrostatic attraction, and functional group bonds depending on how strong intraparticle interactions are, as highlighted in the previous study (Marlina *et al*., 2020). Cd(II) ions adsorption reached the equilibrium stage when the intraparticle interactions stopped, and the biosorbent adsorption capacity remained steady for the rest of the contact time.

Effect of biosorbent size

As highlighted previously, the biosorbent which had more porosity should have more diffusion of adsorbate in the aqueous phase to the solid phase. Consequently, the BIPS-A (less than 0.063 mm) had the highest adsorption capacity, the adsorption capacity of BIPS-B was higher than the BIPS-B and BIPS-C, and the BIPSC had the smallest adsorption capacity. This finding was also reinforced by the previous study for lead ion adsorption by sawdust biosorbent in a size range of 1.18-2.36 mm (Nnaji and Emefu, 2017). The adsorption of Cd, Pb, and Cr ions by eucalyptus activate carbon in a size range of 0.063 to 1,2 mm (Gebretsadik *et al*., 2020) with the maximum adsorption capacity at the size of 0.063 mm, which was the same size as the BIPS-A. These results are reasonable because less size of adsorbent should be more surface area for the diffusion of heavy metal ions on the adsorbent and inside of adsorbent pores (Karau *et al*., 1997, Liese and Hilterhaus, 2013).

Effect of pH

As discussed on the effect of biosorbent size wherein the BIPS-A showed the highest adsorption capacity compared to other biosorbents, then this section only highlighted the effect of pH on the BIPS-A adsorption capacity. The binding of Cd(II) ions with functional groups showed in Figure 1 should be pHdependent. It inclined linearly with the increase of pH, and the highest adsorption capacity was found at pH 5. The reason for this trend might be because lower pH created more hydrogen and hydronium ions to compete Cd(II) ions to be adsorbed on the BIPS-A. These views were supported by previous studies (Lee and Davis, 2001, Luef *et al*., 1991). In addition, the BIPS-A might become more positively charged, resulting in less attraction between Cd(II) ions and BIPS-A, leading to less adsorption (Aldov *et al*., 1995). However, Cd(II) ions adsorption on some adsorbents started decreasing from a pH of 6 (Givianrad *et al*., 2013).

Effect of initial Cd(II) ions concentration

This section considered the effect of initial Cd(II) ions concentration on the BIPS-A adsorption capacity only because of the same reason highlighted in the previous discussion. In general, more adsorbate presented in the solution should give more diffusion of adsorbate onto the adsorbent surface and pores (Marlina *et al*., 2020). Therefore, the adsorption capacity of BIPS-A should increase with the increase in initial Cd(II) ions concentration for the range of initial adsorbate. It has not been reaching a saturation yet, because there should be not enough Cd(II) ions to be occupied by active sites on the BIPS-A even if the initial Cd(II) ions concentration was 662.77 mg/L. It is expected to remain nearly unchanging and saturate for more adsorbate in the solution by increasing the initial concentration of adsorbate (Liu *et al*., 2014, Muslim *et al*., 2017a).

Adsorption kinetic and isotherm

The effect of dependent variables was investigated in the previous discussion. As a result, the highest Cd(II) ions adsorption was 29.513 mg/g under an optimal condition as initial Cd(II) ions concentration of 662.77 mg/L, 1 g dose of the BIPS-A, 80-min contact time, pH 5, 75 rpm of stirring speed, 1 atm, and 30 °C. Therefore, a set of data presenting the optimal condition was chosen for the adsorption kinetic study, which was presented in Figure 3(a), particularly the BIPS-A data. As shown by the R^2 values in Figures 5(a) and 5(b), the gap between Lagergren and Ho R^2 values is not large, which might indicate that the adsorption occurred because of were adsorbed physicochemical interactions between the BIPS-A and Cd(II) ions. However, chemisorption might control more Cd(II) ions adsorption on the BIPS-A due to the PSO kinetic gave the better fitting (0.996) for Cd(II) ions adsorption, which is supported by the previous studies (Wang *et al*., 2007). Using the slope and intercept of Figures 5(b), the adsorption capacity and rate were determined to be approximately 44.444 mg/g and 0.097 g/mg—Min, respectively.

A set of data presenting the optimal condition was also selected for the adsorption isotherm study, which was presented in Figure 4(b). As confirmed by the R^2 values, the Langmuir isotherm was favorable ($R^2 = 0.997$) for Cd(II) ions adsorption by the BIPS-A with the monolayer adsorption capacity and pore volume being 30.121 mg/g and 0.129 L/mg, respectively. Expected in the FTIR discussion, the functional groups on the BIPS-A, which are the O-H; C-H; C=O, and C-O stretches, would be the active sites for chemical adsorption taking place in monolayer with each stretch. The binding energy for each functional group should be equal (Marlina *et al*., 2020). The Langmuir isotherm should be reasonable as expected in the previous adsorption kinetics discussion, whereas chemisorption might control more Cd(II) ions adsorption and a previous study (Muslim *et al*., 2017a).

Conclusion

This study proposed biosorbent from Ipomoea pes-caprae stems (BIPS). The BIPS was prepared economically by drying and grounding. Among the three types of BIPS, the BIPS-A (size being more than 230 mesh) showed the maximum Cd(II) ions adsorption capacity, which was also supported by the best morphological characteristics analyzed using the SEM. Investigation on the adsorption over contact time, adsorbent size, pH, and initial concentration on the Cd(II) ions adsorption capacity of the BIPS resulted in an optimum condition where the system set with 1 g of BIPS-A, 662.77mg/L of initial aqueous Cd(II) ions concentration, pH 5, 1 atm and 30 o C, and the maximum adsorption capacity obtained was 29.513 mg/g. The pseudo-second-order kinetics was more acceptable to present Cd(II) ions adsorption with the correlation coefficient (R 2) of 0.996, and adsorption isotherm fitted very well Langmuir isotherm with the R 2 of 0.997. These results confirmed chemical adsorption of Cd(II) ions might take place more on the biosorbent active sites of OH; C-H; C=O, and C-O stretch.

Acknowledgment

The authors wish to express our profound gratitude to the Chemical Process Laboratory in the Chemical Engineering Department, conduct this research and the FT-IR analysis and Mechanical Engineering Department for the SEM analysis at the Faculty of Engineering, Universitas Syiah Kuala. The authors are also grateful to the Integrated Coastal Resource Management Magister Study Program, Postgraduate Program, Universitas Syiah Kuala for administration support, Faculty of Mathematics and Science, Universitas Syiah Kuala for technical support of the AAS analysis.

References

Aldov, I., Fourest, E., Volesky, B. 1995. Desorption of cadmium from algal biosorbent. The Canadian Journal of Chemical Engineering, 73: 516-522.

Anastopoulos, I., Massas, I., Ehaliotis, C. 2015. Use of residues and by-products of the olive-oil production chain for the removal of pollutants from environmental media: a review of batch biosorption approaches. Journal of Environmental Science and Health—Part, 50(7): 677-18.

Batiga, S., Valli, M., Zeraik, M.L., Fraige, K., Leme, G.M., Pitangui, N.S., Almeida, A.M.F. Michel, S., Young, M.C.M., Bolzani, V.S. 2019. Chemical composition and biological properties of Ipomoea procumbens. Revista Brasileira de Farmacognosia, 29(2): 191-197.

Chakravarty, P., Sarma, N.S., Sarma, H.P. 2010. Removal of lead(II) from aqueous solution using heartwood of Areca catechu powder. Desalination, 256: 16-21.

Cutillas-Barreiro, L., Paradelo, R., Igrexas-Soto A. 2016. Valorization of biosorbent obtained from a forestry waste: competitive adsorption, desorption and transport of Cd, Cu, Ni, Pb and Zn. Ecotoxicology and Environmental Safety, 131: 118-126.

Dimple, L. 2014. Adsorption of Heavy Metals: A Review. International Journal of Environmental Research and Development, 4(1): 41-48.

Dominggus, R. 2011. Concentration of Cadmium Heavy Metals in Water, Sediments and Deadema setosum (Echinoderms, Echinoidea) in Ambon Island Waters. Marine Sciences, 16 (2): 78-85.

Gebretsadik, A., Gebrekidan, A., Demlie, L. 2020. Removal of heavy metals from aqueous solutions using Eucalyptus Camaldulensis: An alternate low cost adsorbent. Cogent Chemistry, 6: 1-16.

Givianrad, M.H., Rabani, M., Saber-Tehrani, M., Aberoomand-Azar, P., Hosseini Sabzevari, M. 2013. Preparation and characterization of nanocomposite, silica aerogel, activated carbon and its adsorption properties for Cd (II) ions from aqueous solution. Journal of Saudi Chemical Society, 17(3): 329-335.

Hernandez-Carlos, B., Bye, R., Pereda-Miranda, R. 1999. Orizabins V–VIII, tetrasaccharide glycolipids from the Mexican scammony root (Ipomoea orizabensis). Journal of Natural Products, 62: 1096-1100.

Karau, A., Benken, C., Thommes, J., Kula M.R. 1997. The influence of particle size distribution and operating conditions on the adsorption performance in fluidized beds. Biotechnology and Bioengineering, 55: 54-64.

Kozak, L., Kokociński, M., Niedzielski, P., Lorenc, S. 2015. Bioaccumulation of metals and metalloids in medicinal plant Ipomoea pes-caprae from areas impacted by tsunami. Environmental Toxicology and Chemistry, 34(2): 252-257.

Kurniawan, T.A., Chan, G.Y.S., Lo W.H., Babel, S. 2006. Comparisons of low-cost adsorbents for treating wastewaters laden with heavy metals. Science of The Total Environment, 366(2–3): 409-426.

Lee, C.L., H'ng, P.S., Paridah, M.T., Chin, K.L., Rashid, U., Maminski, M., Go, W.Z., Nazrin, R., Rosli, S., Khoo, P.S. 2018. Production of bioadsorbent from phosphoric acid pretreated palm kernel shell and coconut shell by two-stage continuous physical activation via N_2 and air. Royal Society open science, 5(12): 1-19.

Lee, H.W., Insyani, R., Prasetyo, D., Prajitno, H., Sitompul, J.P. 2015. Molecular Weight and Structural Properties of Biodegradable PLA Synthesized with Different Catalysts by Direct Melt Polycondensation. Journal of Engineering and Technological Sciences, 47(4): 364-373.

Lee, S.M., Davis A.P. 2001. Removal of Cu(II) and Cd(II) from aqueous solution by seafood processing waste sludge. Water Research, 35: 534-540.

Luef, E., Prey, T., Kubicek, C.P. 1991. Zinc biosorption by fungal waste mycelia. Applied Microbiology and Biotechnology, 34: 688-692.

Liese, A., Hilterhaus, L. 2013. Evaluation of immobilized enzymes for industrial applications. Chemical Society Reviews, 42: 6236-6249.

Liu, X., Zhang, W., Zhang, Z. 2014. Preparation and characteristics of activated carbon from waste fiberboard and its use for adsorption of Cu(II). Materials Letters, 116: 304-306.

Mahmood-ul-Hassan, M., Suthor, V., Rafique, E., Yasin, M. 2015. Removal of Cd, Cr, and Pb from aqueous solution by unmodified and modified agricultural wastes. Environmental Monitoring and Assessment, 187(2): 19-26.

Marlina, Iqhrammullah, M., Saleha, S., Fathurrahmi, Fandini Putri Maulina, F.P., Idroes, R. 2020. Polyurethane film prepared from ball-milled algal polyol particle and activated carbon filler for NH3–N removal. Heliyon, 6(8): e04590.

Medhi, H., Chowdhury, P.R., Baruah, P.D., Bhattacharyya, K.G. 2020. Kinetics of Aqueous Cu(II) Biosorption onto Thevetia peruviana Leaf Powder. ACS Omega, 5(23): 13489-13502.

Mengistie, A.A., Siva, R.T., Prasada, R.A.V., Singanan, M. 2008. Removal of lead(II) ion from aqueous solution using activated carbon from Militia ferruginea plant leaves. Bulletin of the Chemical Society of Ethiopia, 22(3): 349-360.

Muslim, A. 2017. Australian pine cones-based activated carbon for adsorption of copper in aqueous solution. Journal of Engineering Science and Technology, 12(2): 280-295.

Muslim, A., Aprilia, S., Suha, T.A., Fitri, Z. 2017a. Adsorption of Pb (II) ions from aqueous solution using activated carbon prepared from areca catechu shell: Kinetic, isotherm and thermodynamic studies. Journal of the Korean Chemical Society, 61(3): 89-96.

Muslim, A., Ellysa, Said, S.D. 2017b. Cu(II) Ion Adsorption Using Activated Carbon Prepared from Pithecellobium Jiringa (Jengkol) Shells with Ultrasonic Assistance: Isotherm, Kinetic and Thermodynamic Studies. Journal of Engineering and Technological Sciences, 49(4): 472-490.

Muslim, A., Zulfian, Ismayanda, M.H., Devrina, E., Fahmi, H. 2015. Adsorption of Cu(II). from the aqueous solution by chemical activated adsorbent of areca catechu shell. Journal of Engineering Science and Technology, 10(12): 1654-1666.

Nahar, K., Chowdhury, Md.A.K., Chowdhury, Md.A.H., Rahman, A., Mohiuddin, K. M. 2018. Heavy metals in handloom-dyeing effluents and their biosorption by agricultural byproducts. Environmental Science and Pollution Research, 25(8): 954-7967.

Nnaji, C.C., Emefu, S.C. 2017. Effect of particle size on the sorption of lead from water by different species of sawdust: Equilibrium and kinetic study. BioResources, 12(2): 4123-4145.

Pareda-Miranda, R., Escalanate-Sanchez, E., Escobeda-Martinez, C. 2005. Characterization of lipophilic pentasaccharides from beach morning glory ipomoea pes-caprae. Journal of Natural Products, 56(12): 1724-1726.

Teramachi, F., Koyano, T., Kowithayakor, T., Hayashi, M., Komiyama, K., Ishibashi, M. 2005. Collagenase inhibitory quinic acid ester from Ipomoea pes-caprae. Journal of Natural Product, 68: 794-796.

Wan, L., Zhang H. 2012. Cadmium toxicity: effects on cytoskeleton, vesicular trafficking and cell wall reconstruction. Plant Signaling & Behavior, 7(3): 345-348.

Wang, H., Zhou, A., Peng, F., Yu, H., Yang, J. 2007. Mechanism study on adsorption of acidified multi-walled carbon nanotubes to Pb(II). The Journal of Colloid and Interface Science, 316: 277-283.

Wong, K.K., Lee, C.K., Low, K.S., Haron, M.J. 2003. Removal of Cu and Pb by tartaric acid modified rice husk from aqueous solution. Chemosphere, 50, 23-28.

Rao, K. S., Mohapatra, M., Anand, S., Venkateswarlu, P, 2010. Review on cadmium removal from aqueous solutions. International Journal of Engineering. Science and Technology, 2(7): 81-103.

Rosas-Ramírez, D., Pereda-Miranda, R. 2013. Resin glycosides from the yellow-skinned variety of sweet potato (Ipomoea batatas). Journal of Agricultural and Food Chemistry, 61: 9488-9494.

Venkataraman, D. N., Atlee, C. W., Prabhu, P. T. 2003. Phyto Chemical analysis from ipomoea pes-caprae. International Research. Journals of Pharmaceutical and Applied Sciences, 3(4): 79-83.

Zhang, M., Hu, Z., Wang, H., McDonald L. M. 2017. Competitive biosorption of Pb (II), Cu (II), Cd (II) and Zn (II) using composted livestock waste in batch and column experiments. Environmental Engineering and Management Journal, 16(2): 431-438.

Zorica, R.L., Mirjana, D.S., Smilja, B.M., Jelena, V.M., Marija, L.M., Tatjana, S.K.R., Mirjana, L.J.K. 2019. Effects of different mechanical treatments on structural changes of lignocellulosic waste biomass and subsequent Cu(II) removal kinetics. Arabian Journal of Chemistry, 12(8): 4091-4103.